Science of Sintering, **49** (2017) 277-284

doi: https://doi.org/10.2298/SOS1703277L

UDK 543.42, 621.926.087

Yttrium Orthoferrite Powder Obtained by the Mechanochemical Synthesis

Zorica Ž. Lazarević[1,*)], Čedomir Jovalekić[2], Martina Gilić[1], Valentin Ivanovski[3], Ana Umićević[3], Dalibor Sekulić[4], Nebojša Ž. Romčević[1]

[1]Institute of Physics, University of Belgrade, Pregrevica 118, Zemun, Belgrade, Serbia

[2]The Institute for Multidisciplinary Research, University of Belgrade, Belgrade, Serbia

[3]Institute of Nuclear Sciences Vinča, University of Belgrade, Belgrade, Serbia

[4]Faculty of Technical Sciences, University of Novi Sad, Novi Sad, Serbia

Abstract:

Yttrium orthoferrite ($YFeO_3$) powder was prepared by a mechanochemical synthesis from a mixture of Y_2O_3 and α–Fe_2O_3 powders in a planetary ball mill for 2.5 h. The obtained $YFeO_3$ powder sample was characterized by X–ray diffraction (XRD), Raman and infrared spectroscopy. The average crystallite size calculated by the Scherrer equation was 12 nm. The Mössbauer spectroscopy at room temperature confirms the superparamagnetic character of $YFeO_3$ orthoferrite sample.

Keywords: *$YFeO_3$; Raman spectroscopy; IR spectroscopy; Mössbauer spectroscopy.*

1. Introduction

In the past few years, a renewed interest has grown in the study of orthorhombically distorted perovskites. An important example of this trend is the family of orthoferrites, with a general formula $R\mathrm{FeO_3}$, where R is the trivalent rare-earth metal ion or yttrium [1]. Orthoferrites have been extensively studied for their physical properties and potential applications [2-4]. These materials are of considerable interest on account of their novel magnetic, optical and magneto–optical properties [5]. Also, Y and rare–earth orthoferrites exhibit interesting physical and chemical properties because of their ionic and electronic defects [6, 7]. However, systematic spectroscopic investigations of orthoferites have not been done jet. Reviewing the literature, one can find the analysis of Raman spectra rare–earth orthoferrites [8] and $\mathrm{YFeO_3}$ [15], but far and mid IR reflectivity measurements are not available.

The family of orthorhombically distorted perovskites have the same *Pnma* space group and 4 formula units per unit cell [8-11]. The basic building units of orthoferrites are $\mathrm{FeO_6}$ octahedral that are corner–connected along the *b* axis. Four corner–connected oxygen atoms, O1, and additional charge balancing yttrium cations, which occupy interstitial positions between octahedral, are in ***4c*** Wyckoff–site with C_s^{xz} symmetry (Fig. 1). The eight

*) **Corresponding author:** lzorica@yahoo.com

oxygen atoms (O2) found in the ac plane occupy Wyckoff positions ***8d*** and possess site symmetry *C1*. According to the recent inelastic neutron scattering measurements the lattice constants of $YFeO_3$ single crystal, are a = 5.282Å, b = 7.605 Å, and c = 5.596 Å [12]. Below 640 K, $YFeO_3$ is a noncollinear antiferromagnet [12, 13]. The direct interaction between nearest neighbour Fe magnetic moments in yttrium and rare–earth orthoferrite crystals is negligible. The spins are coupled through the oxygen atoms by the super exchange mechanism. This interaction is predominantly antiferromagnetic with an anti-symmetric component (Dzyaloshinsky–Moriya anti–symmetric exchange [14]) which causes a slight canting of the moments of adjacent iron atoms and a resultant weak ferromagnetic moment as well.

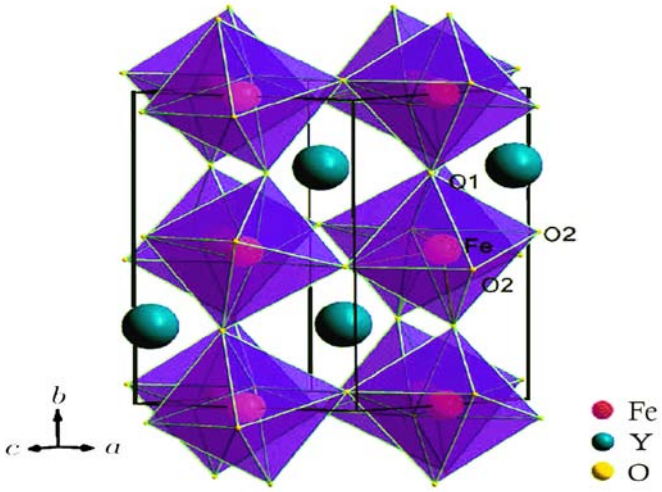

Fig. 1. Structure of $YFeO_3$.

The usual method for synthesizing such compounds, viz. by sintering stoichiometric mixtures of the rare-earth oxide (R_2O_3) and Fe_2O_3 is unsuitable in this case because it leads to the formation of garnets as well as orthoferrites at low temperatures. Most of mentioned approaches for synthesis of single phase perovskite $YFeO_3$ require the calcination process at high temperature around 1173 K, which results in energy and time consumption usually associated to multistage synthesis [15].

Rare–earth orthoferrites are often prepared from high temperature solid-state reactions of the corresponding pure oxides [16]. However, this process suffers from problems such as excessive crystal growth, irregular atomic stoichiometric ratio, and formation of undesirable phases. Polycrystalline rare–earth orthoferrites ($RFeO_3$) and iron garnets ($R_3Fe_5O_{12}$) are usually prepared by sintering mixtures of rare earth oxide (R_2O_3) and Fe_2O_3 at elevated temperatures (> 1300 °C). This method, however, often involves the formation of impurity phases such as garnets (in the orthoferrites) and magnetite. Multiple firings are usually necessary to obtain materials which are single phase with respect to XRD measurements. On the other hand, Racu and co-authors [17] present a new, fast and high yield synthesis method for obtaining microcrystalline $YFeO_3$ orthoferrite, based on hydrothermal technique. The advantage of the method consists in the direct crystallization of the material without the necessity of the calcination. Other synthesis routes have also been proposed including the precipitation method, thermal decomposition process, solvothermal treatment, sonochemical approach, combustion route, alkoxide method and solid state reaction [18-24].

Mechanical activation is a very effective method for obtaining a highly dispersed system as mechanical action stress fields form in solids during the milling procedure [25]. During milling, heat is released, new surfaces and different crystal lattice defects are formed and a solid-state reaction is initiated. The accumulated deformation energy is the key of

understanding the route of irreversible changes of the crystal structure and consequently microstructure, causing changes of material properties [25]. In many cases, the mechanical activation is superior to the conventional solid-state reaction for the ceramic powder preparation for several reasons. It uses low–cost and widely available oxides as starting materials and skips the calcinations step at an intermediate temperature, conducting to simplified process [26].

In this work, we were investigated the nanocrystalline $YFeO_3$ powder obtained by the mechanochemical synthesis in a planetary ball mill. The mechanochemical reaction leading to formation of the $YFeO_3$ phase was followed by XRD, Raman and IR spectroscopy. The Mössbauer spectroscopy at room temperature confirms the superparamagnetic character of $YFeO_3$ orthoferrite sample.

2. Experimental procedures

The starting material were: yttrium (III)–oxide (Y_2O_3, Alfa Aesar 99.9 % purity) and hematite (α–Fe_2O_3, Merck 99 % purity). Mechanochemical synthesis was performed in air atmosphere in planetary ball mill (Fritsch Pulverisette 5).

Characterization of the sample obtained after 2.5 h milling time was carried out by several methods.

• XRD analysis was performed on X-ray diffractometer (Rigaku Corporation, Japan) at room temperature. CuKα radiation (λ = 0.15418 nm) with a step size of 0.01° in the range of 2θ = 10-80° was used. The peaks were identified using the Powder Diffraction File (PDF) database created by International Centre for Diffraction Data (ICDD).

• The micro-Raman spectra were taken in the backscattering configuration and analyzed by Jobin Yvon T64000 spectrometer, equipped with nitrogen cooled charged coupled device detector. As an excitation source the 532 nm line of Ti was used: Sapphire laser, with laser power 20 mW. The measurements were performed in the spectrum range 100 – 800 cm^{-1}.

• The infrared (IR) measurements were carried out with a BOMMEM DA–8 FIR spectrometer. A DTGS pyroelectric detector was used to cover the wave number range 50 – 700 cm^{-1}.

• The measurements of the Mössbauer effect in $YFeO_3$ nanocrystalline powder were performed in a transmission geometry using a ^{57}Co(Rh) source at the room temperature (RT). The spectra have been examined by WinNormos–Site or WinNormos–Dist/Xls software packages [27]. The former is based on the least squares method whereas the latter combines distribution of Lorentz lines and subspectra based on the histogram and the least squares method, respectively. The Wissel spectrometer was calibrated by the spectra of natural iron foil. Sample thickness correction was carried out by a transmission integral. Isomer shift values are in reference to a metallic alpha iron (δ = 0).

3. Results and discussions

Fig. 2 presents the XRD pattern of: the starting mixture after 2.5 h of milling. Obtained diffractogram is compared with the data from the Powder Diffraction Files: PDF#39–1489 for yttrium orthoferrite, PDF#33–0664 for hematite and PDF#41–1105 for yttrium (III) oxide. After 2.5 h of milling the orthorhombic distorted perovskite structure with space group of *Pnma* become dominant. Only a few percents of Y_2O_3 and Fe_2O_3 indicate that the reaction is practically completely finished.

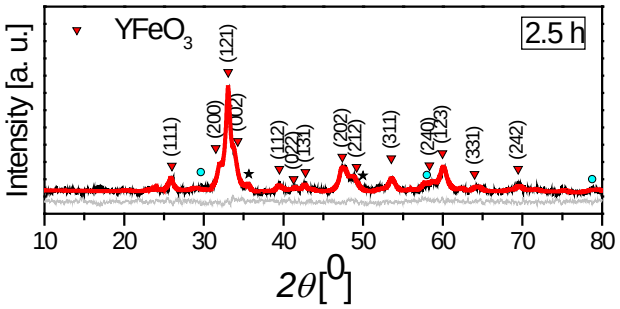

Fig. 2. XRD pattern of $YFeO_3$ orthoferrite obtained from the mixture of Y_2O_3 and α–Fe_2O_3 powders after 2.5 h milling time (symbols in red ∇ – $YFeO_3$; blue • – Fe_2O_3; black ∗ – Y_2O_3 are assigned to identified phases).

The crystallite size (S) of $YFeO_3$ powder mechanochemically treated for 2.5 h was calculated by means of Scherrer equation [28-30] using XRD data for the most prominent (121) Bragg reflection as:

$$S = 0.9\,\lambda / (\beta \cos\theta) \quad (1)$$

where λ – X–ray wavelength, β – full width at half–maximum, θ – Bragg angle. Estimated average crystallite size is 12 nm.

The group theory [31-33] predicts 60 vibration modes at the centre of Brilouin zone: $\Gamma = 7A_g + 8A_u + 5B_{1g} + 10B_{1u} + 7B_{2g} + 8B_{2u} + 5B_{3g} + 10B_{3u}$. Therefore, for unpolarised spectra of a polycrystalline sample, we would expect at most 24 Raman bands ($7A_g + 5B_{1g} + 7B_{2g} + 5B_{3g}$) and 25 infrared–active ones ($9B_{1u} + 7B_{2u} + 9B_{3u}$), $8(8A_u)$ are silent, and $3(B_{1u} + B_{2u} + B_{3u})$ are acoustic modes.

Unpolarised Raman spectra presented in Fig. 3 are excited by laser line λ= 532 nm and recorded in backscattering geometry at room temperature. As Fe atoms are in centre of symmetry they do not participate in Raman active modes. The corresponding modes in different orthorhombically distorted perovskites with symmetry *Pnma* are not different too much. So we could assign modes in our Raman spectra of nanosized $YFeO_3$ in accordance with literature data [8, 34, 35]. We observed all 7 A_g modes at 146, 177.5, 289, 335, 405, 494 and 525 cm^{-1}. Two strong B_{2g} modes are at 221 and 608 cm^{-1} and one B_{1g} at 434 cm^{-1}. The origin of a strong wide feature at 655 cm^{-1} arises from two-phonon process and probably due to crystal disorder. In the Raman spectra of single crystals this band is hardly visible [8, 35], but in the spectra of polycrystalline samples is much exaggerated. Mandal at al. [36] deconvoluted this band (at 648 cm^{-1} in $YFe_{0.6}Mn_{0.4}O_3$) and found that at this energy there are two (second order) phonons with different symmetries – B_{2g} and B_{3g}.

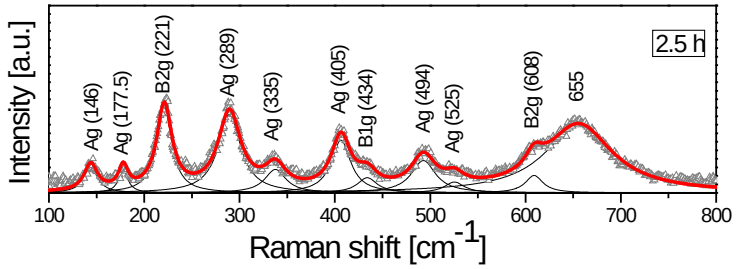

Fig. 3. Raman spectrum of $YFeO_3$ orthoferrite obtained from the mixture of Y_2O_3 and α–Fe_2O_3 powders after 2.5 h milling time at room temperature.

Infrared reflectivity spectrum of the practically pure $YFeO_3$ phase after 2.5 h of milling is presented in Fig. 4. A number of modes that can be related to an $YFeO_3$ phase are visible. As a result of the best fit we obtained 10 modes with parameters listed in Fig. 4.

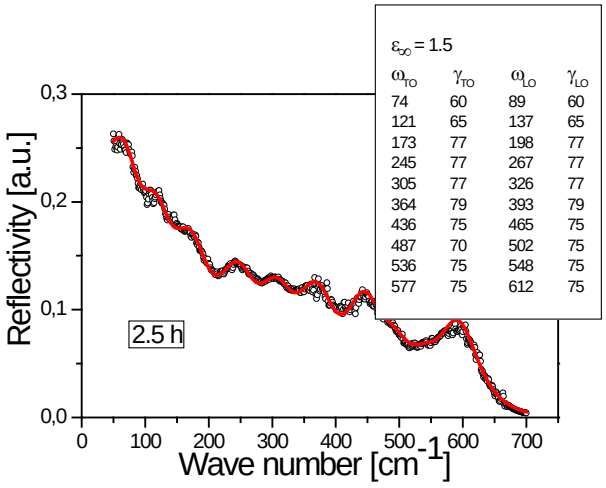

Fig. 4. IR spectrum of $YFeO_3$ orthoferrite obtained from the mixture of Y_2O_3 and α–Fe_2O_3 powders after 2.5 h milling time at room temperature.

To the best of our knowledge, about the reflectivity measurements of $YFeO_3$ in the far and mid infrared range in literature and only two references have reported the transmittance of $YFeO_3$, but in the range of wave numbers higher than 400 cm^{-1}. This assertion can be seen in the works that show investigation nanocrystals of $YFeO_3$ obtained by sol-gel auto-combustion process [37] and sintered samples (as a part of investigation of $YFe_{1-y}Mn_yO_3$) [38]. Comparing theoretical [31, 33, 39] and experimental data for IR modes from available literature, together with results obtained by fitting procedure in this work, we can conclude that IR modes of various orthoferrites are very close, even modes of orthoferrite and orthomanganite, as has already been shown for Raman modes. IR modes generally can be assigned to three different types of motion (came up from splitting of modes in ideal perovskite structure): 1)Y (or rare–earth) – external modes at the lowest frequencies, 2) Fe-O bending modes in the intermediate range from 270 cm^{-1} to 500 cm^{-1}, and 3) oxygen stretching modes at higher frequencies. Considering that our nanosized samples are obtained by ball milling (mechanochemical reaction) it is possible that the presence of numerous defects, like disturbed octahedrons, can result in broadening of modes, or even arising of new modes. We suppose that merged modes centered at about 570 cm^{-1} correspond to stretching vibration(s). The strongest mode at 436 cm^{-1} is a little lower than reported [37, 38]. All other lower energy modes can be compared only with modes of some other compounds with the same *Pnma* structure, or with theoretically obtained values for rare–earth orthoferrites [32] and lanthanum orthomanganite [33, 39]. It can be concluded that the first fitted mode at ω_{TO} = 74 cm^{-1} (ω_{LO} = 89 cm^{-1}) has B_{1u} symmetry. Rather broad mode 121(137) cm^{-1} can be a combination of two close modes B_{1u} and B_{3u}. Modes at 173(198) cm^{-1} and 245(267) cm^{-1} have symmetry B_{1u} and B_{2u}, respectively. Those are so called external modes, mixed vibrations of Y and octahedra FeO_6. The higher frequency modes do not involve motions of Y atoms, but only vibrations of O–Fe–O bond in octahedra. The second group of phonons with frequencies lying between 270 and 500 cm^{-1} is expected to originate from splitting of the bending mode of the ideal perovskite structure. These are modes B_{3u} at 305(326) cm^{-1}, B_{1u} at 364(393) cm^{-1}, B_{1u} at 436(465) cm^{-1} and B_{3u} at 487(502) cm^{-1} (Fig. 4). In the third group are stretching modes B_{3u} at 536(548) cm^{-1} and strong B_{2u} at 577(612) cm^{-1}. Even though if we were not able to assign all IR modes, at least two most prominent modes (B_{1u} at 436(465) cm^{-1} and B_{2u} at 577(612) cm^{-1}) confirm that after 2.5 h of milling orthoferrite *Pnma* structure is obtained.

The Mössbauer spectrum (Fig. 5) obtained for 2.5 h milled sample is resolved by five sextets and three doublets. The sextet with the hyperfine interaction parameters which

correspond to hematite is clearly identified. Its relative amount is 6.0(3) %. The remaining four sextets are recognized to represent response from the yttrium orthoferrite. The relative amount of well crystallized large particles is 16(2) %. The other three sextets that follow the reduction of particles´ volume are in accordance with the findings of Modi et al., i.e. hyperfine field magnitude and isomer shift values decrease with decreasing particle size or increasing milling time [40]. Two superparamagnetic doublets show that further milling produced additional more than 10% small sized particles. Pinkas et al. reported the measured isomer shift value of 0.34 mm s^{-1} and quadrupole splitting of 0.79 mm s^{-1} for the amorphous $YFeO_3$ at 300 K [41]. These results are in agreement with the parameters of doublet obtained in our measurement. The doublet with the largest quadrupole splitting value of 2.32(1) mm s^{-1} provokes the most doubts in interpretation. The $YFeO_3$ with hexagonal structure is a metastable phase. There is only one non-equivalent Fe site in hexagonal $YFeO_3$ whereas the observation of two Fe sites in this phase was related to the small crystallites of the Fe–rich compound [42, 43]. The reported hyperfine parameters for these two Fe sites at room temperature are 2.13(2) and 1.18(2) mm s^{-1} for the quadrupole splitting and the isomer shift of 0.29(2) and 0.30(2) mm s^{-1}, respectively. The ratio of relative area is 4:3 [44]. The relative amount of the doublet is probably under detection limit of XRD as an aggravating circumstance. Taking into account that our parameters do not entirely match the cited values, while partially agree with the ones of Modi et al. [40], this doublet is attributed to the smallest $YFeO_3$ particles. The creation of oxygen vacancies during milling might have reduced some of the Fe^{3+} ions to Fe^{2+} ions [40]. The distinctive isomer shift high value was not identified in our spectra. Thus, we conclude that the yttrium orthoferrite represents 94 % of the sample obtained after 2.5 h milling time. After normalization with respect to the yttrium orthoferrite amount, the following distribution of particle size is obtained: 17 % large, 38 % medium sized and 45 % small particles.

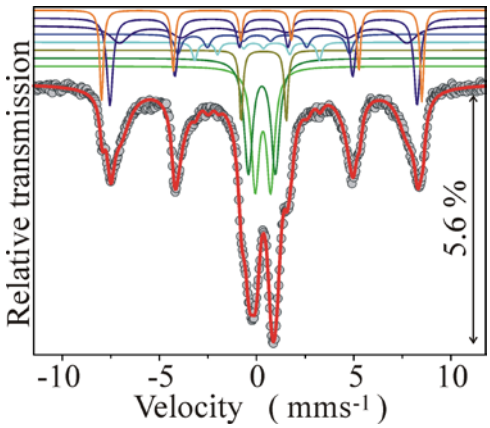

Fig. 5. Mössbauer spectrum at T = 294 K of $YFeO_3$ orthoferrite obtained from the mixture of Y_2O_3 and α–Fe_2O_3 powders after 2.5 h milling time. The experimental data are presented by solid circles and the fit is given by the red solid line. Vertical arrow denotes relative position of the lowermost peak with respect to the basal line. The fitted lines of subspectra are plotted above the main spectrum fits.

4. Conclusions

Nanosized yttrium orthoferrite ($YFeO_3$) powder was synthesized by mechanochemical treatment of Y_2O_3 and α–Fe_2O_3 mixture in planetary ball mill for 2.5 h. XRD shows that yttrium orthoferrite structure is dominant in the form of fine crystallites with average size 12 nm. The eleven Raman active modes are observed in first-order Raman

spectra at the room temperature. An IR reflectivity spectrum is fitted by 10 modes. Mössbauer measurement analysis shows that the dominant part of the yttrium orthoferrite phase are small and medium sized nanoparticles. After 2.5 h of milling the mixture contains 6 % of unreacted hematite.

Acknowledgments

This research was financially supported by the Ministry of Education, Science and Technological Development of the Republic of Serbia through Projects No. III 45003 III 45015, III 45018 and research project under the agreement of scientific collaboration between Polish Academy of Science and Institute of Physics Belgrade.

5. References

1. N. Singh, J. Y. Rhee, J. Korean Phys. Society, 53 (2008) 806-811.
2. Y. S. Didosyan, H. Hauser, H. Wolfmayer, J. Nicolics, P. Fulmek, Sens. Actuators A, 106 (2003) 168-171.
3. Y. S. Didosyan, H. Hauser, W. Toriser, Int. J. Appl. Electrom., 13 (2001) 277-283.
4. P. Ripka, G. Vértesy, J. Magn. Magn. Mater., 215-2016 (2000) 795-799.
5. A. R. Akbashev, A. S. Semisalova, N. S. Perov, A. R. Kaul, Appl. Phys. Lett., 99 (2011) 122502.
6. E. Traversa, P. Nunziante, L. Sangaletti, B. Allieri, L. E. Depero, H. Aono, Y. Sadaoka, J. Am. Ceram. Soc., 83 (2000) 1087-1092.
7. M. Cherry, M. S. Islam, C. R. A. Catlow, J. Solid State Chem., 118 (1995) 125-132.
8. S. Venugopalan, M. Dutta, A. K. Ramdas, J. P. Remeika, Phys. Rev. B, 31 (1985) 1490-1497.
9. M. Derras, N. Hamdad, Results in Physics, 3 (2013) 61-69.
10. P. Coppons, M. Eibschutz, Acta Crystallogr., 19 (1965) 524-531.
11. M. Marezio, J. P. Remeika, P. D. Derrier, Acta Crystallogr. B, 26 (1970) 2008-2022.
12. S. E. Hahn, A. A. Podlesnyak, G. Ehlers, and G. E. Granroth, R. S. Fishman, A. I. Kolesnikov, E. Pomjakushina, K. Conder, Phys Rev B, 89 (2014) 014420.
13. R. Nirat, V. W. Umesh, Phys.Rev. B, 77 (2008) 134112-134121.
14. I. Dzyaloshinsky, J. Phys. Chem. Solids, 4 (1958) 241-255.
15. P. Ayyub, M. S. Multani, A. Gurjar, Mater. Lett., 2 (1983) 122-126.
16. A. Sztaniszlav, E. Sterk, L. Fetter, M. Farkas-Jahnke, J. Magn. Magn. Mater., 41 (1984) 75-78.
17. A.V. Racu, D. H. Ursu, O. V. Kuliukova, C. Logofatu, A. Leca, M. Miclau, Mater. Lett., 140 (2015) 107-110.
18. S. Nakayama, J. Mater. Sci., 36 (2001) 5643-5648.
19. D. S. Todorovsky, R. V. Todorovska, St. Groudeva-Zotova,Mater. Lett., 55 (2002) 41-45.
20. M. Inoue, T. Nishikawa, T. Nakamura, T. Inui, J. Am. Ceram. Soc., 80 (1997) 2157-2160.
21. M. Sivakumar, A. Gedanken, W. Zhong, Y. H. Jiang, Y. W. Du, I. Brukental, D. Bhattacharya, Y. Yeshurun, I. Nowik, J. Mater. Chem., 14 (2004) 764-769.
22. Q. Ming, M. D. Nersesyan, A. Wagner, J. Ritchie, J. T. Richardon, D. Luss, A. J. Jacobson, Y. L. Yang, Solid State Ionics, 122 (1999) 113-121.
23. Y. Matsuura, S. Matsushima, M. Sakamoto, Y. Sadaoka, J. Mater. Chem., 3 (1993) 767-769.
24. J. G. McCarty, H. Wise, Catal. Today, 8 (1990) 231-248.

25. M. M. Vijatović, J. D. Bobić, B. D. Stojanović, Sci. Sinter., 40 (2008) 155-165.
26. Z. Ž. Lazarević, B. D. Stojanović, M. J. Romčević, N. Ž. Romčević, Sci. Sinter., 41 (2009) 19-26.
27. R. A. Brand, WinNormos Mössbauer fitting program. Universität Duisburg (2008).
28. V. I. Popkov, O. V. Almjasheva, V. N. Nevedomskiy, V. V. Sokolov , V. V. Gusarov, Nanosyst.: Phys., Chem., Math., 6 (2015) 866-874.
29. A. Patterson,Phys. Rev., 56 (1939) 978-982.
30. Z. Ž. Lazarević, Č. Jovalekić, D. Sekulić, M. Slankamenac, M. Romčević, A. Milutinović, N. Ž. Romčević, Sci. Sinter., 44 (2012) 331-339.
31. M. A. Islam, J. M. Rondinelli, J. E. Spanier, J. Phys.: Condens. Matter., 25 (2013) 175902.
32. H. C. Gupta, M. K. Singh, L. M. Tiwari, J. Raman Spectrosc., 33 (2002) 67-70.
33. I. S. Smirnova, Physica B, 262 (1999) 247-261.
34. M. N. Iliev, M. V. Abrashev, H.-G. Lee, V. N. Popov, Y. Y. Sun, C. Thomsen, R. L. Meng, C. W. Chu, Phys. Rev. B, 57 (1998) 2872-2877.
35. N. D. Todorov, M. V. Abrashev, V. G. Ivanov, G. G. Tsutsumanova, V. Marinova, Y.-Q. Wang, M. N. Iliev, Phys. Rev. B, 83 (2011) 224303.
36. P. Mandal, Venkata Srinu Bhadram, Y. Sundarayya, Chandrabhas Narayana A. Sundaresan, C. N. R. Rao, Phys. Rev. Letters, 107 (2011) 137202.
37. W. Zhang, C. Fang, Wenhui Yin, Y. Zeng, Mat. Chem. Phys., 137 (2013) 877-883.
38. X. Cao, C. S. Kim, H. I. Yoo, J. Am. Ceram. Soc., 84 (6) (2001) 1265-1272.
39. A. Paolone, P. Roy, A. Pimenov, A. Loidl, O. K. Mel'nikov, A. Ya. Shapiro, Phys. Rev. B, 61 (2000) 11255-11258.
40. K. Modi, S. N. Dolia, P. U. Sharma, Indian Journal of Physics, 89 (5) (2015) 425-436.
41. J. Pinkas, V. Reichlova, A. Serafmidisova, Z. Moravec, R. Zboril, D. Jancik, P. Bezdicka, J. Phys. Chem. C, 143 114 (32) (2010) 13557-13564.
42. E. Murad, John Cashion, Mössbauer Spectroscopy of Environmental Materials and their Industrial Utilization, Springer US, Springer Science+Business Media New York, 2004.
43. P. Jiang, J. Li, A. W. Sleight, M. A. Subramanian, Inorg. Chem., 50 (13) (2011) 5858-5860.
44. L. J. Downie, R. J. Goff, W. Kockelmann, S. D. Forder, J. E. Parker, F. D. Morrison, P. Lightfoot, J. Solid State Chem., 190 (2012) 52-60.

Садржај: *Итријум ортоферит ($YFeO_3$) је добијен из смеше прахова Y_2O_3 и α–Fe_2O_3 механохемијском синтезом након 2.5 часа млевења у планетарном млину. Добијени прах $YFeO_3$ је био карактерисан методом рендгенске дифракције, Раман и инфрацрвеном спектроскопијом. Просечна величина кристалита израчуната Шереровом једначином је била 12 nm. Мосбауер спектроскопија на собној температури потврђује суперпарамагнетни карактер узорка $YFeO_3$.*
Кључне речи: *$YFeO_3$; Раман спектроскопија; инфрацрвена спектроскопија; Мосбауер спектроскопија.*